Development 138, 1297-1308 (2011) doi:10.1242/dev.059386
© 2011. Published by The Company of Biologists Ltd

The fibronectin leucine-rich repeat transmembrane protein Flrt2 is required in the epicardium to promote heart morphogenesis

Pari-Sima Müller[1], Ramona Schulz[1,*], Silvia Maretto[1,†], Ita Costello[1], Shankar Srinivas[2], Elizabeth Bikoff[1] and Elizabeth Robertson[1,‡]

SUMMARY

The epicardium, the outermost tissue layer that envelops the developing heart and provides essential trophic signals for the myocardium, derives from the pro-epicardial organ (PEO). Two of the three members of the Flrt family of transmembrane glycoproteins, Flrt2 and Flrt3, are strongly co-expressed in the PEO. However, beginning at around day 10 of mouse development, following attachment and outgrowth, Flrt3 is selectively downregulated, and only Flrt2 is exclusively expressed in the fully delaminated epicardium. The present gene-targeting experiments demonstrate that mouse embryos lacking Flrt2 expression arrest at mid-gestation owing to cardiac insufficiency. The defects in integrity of the epicardial sheet and disturbed organization of the underlying basement membrane closely resemble those described in Flrt3-deficient embryos that fail to maintain cell-cell contacts in the anterior visceral endoderm (AVE) signalling centre that normally establishes the A-P axis. Using in vitro and in vivo reconstitution assays, we demonstrate that Flrt2 and Flrt3 are functionally interchangeable. When acting alone, either of these proteins is sufficient to rescue functional activities in the AVE and the developing epicardium.

KEY WORDS: Flrt proteins, Leucine-rich repeats, Cardiogenesis, Epicardium, Basement membrane, Mouse

INTRODUCTION

The key transcription factors and inductive signalling cues that govern specification of early heart progenitor populations and subsequently drive their expansion and terminal differentiation into muscle and non-muscle cell lineages have been intensively investigated. Three sources of heart progenitors – the cardiogenic mesoderm, neural crest and the pro-epicardial organ (PEO) – are known to contribute to distinct structural components (for reviews, see Srivastava and Olson, 2000; Buckingham et al., 2005; Olson, 2006; Martin-Puig et al., 2008; Vincent and Buckingham, 2010). The earliest cardiogenic mesoderm, formed at embryonic day (E) 7.5, gives rise to the cardiomyocytes of the linear heart tube (E8.5) and subsequently the myocardium of the ventricular and atrial chambers, as well as endocardial endothelial cells. At slightly later stages (E9.5-E10.5), migration of neural crest derivatives into the outflow tract is required for remodelling and separation of the arteries (for a review, see Jiang et al., 2000). The PEO, a cauliflower-like cluster of cells adjacent to the septum transversum, gives rise to the epicardium that attaches and spreads across the surface of the myocardium forming the outermost tissue layer (for a review, see Manner et al., 2001). From mid-gestation onwards, these multipotent cardiac progenitors cooperatively proliferate and diversify to orchestrate the tightly regulated developmental programme that promotes myocardial growth and trabeculation, formation of the coronary vascular system, induction of the endocardial cushions, as well as patterning and septation of the atrial and ventricular chambers.

Relatively little is known about the cell-surface receptors and extracellular matrix (ECM) molecules that guide cell movements and promote tissue contacts during cardiogenesis. The ‘cardiac jelly’ ECM proteins located between the contractile myocardial cells and the inner endocardial cells potentially regulate cell communication, migration and tissue remodelling. Expression of vascular cell adhesion molecule 1 (VCAM1) in the myocardium and its receptor α4β1-integrin in the epicardium is essential for functional tissue associations. In VCAM1-deficient embryos the epicardial cells detach from the surface of the heart. As the epicardium is an important source of trophic factors (for a review, see Lavine and Ornitz, 2009), this loss of tissue integrity secondarily causes hypoplasia of the myocardium and impaired vasculogenesis (Kwee et al., 1995). Similarly, loss of α4β1-integrin disrupts attachment and spreading of epicardial progenitor cells across the surface of the heart, and results in myocardial defects (Yang et al., 1995; Sengbusch et al., 2002).

The present work focuses on potentially unique and shared roles contributed by the fibronectin leucine-rich repeat transmembrane glycoproteins. Three closely related family members (Flrt1-Flrt3), highly conserved across vertebrate evolution (Haines et al., 2006; Bottcher et al., 2004; Smith and Tickle, 2006), share key structural features: 10 leucine-rich repeats (LRR), a type III fibronectin (FN) domain, followed by the transmembrane segment and a short cytoplasmic tail (Lacy et al., 1999). We and others have described *Flrt1*, *Flrt2* and *Flrt3* expression patterns in the developing mouse embryo (Haines et al., 2006; Maretto et al., 2008). *Flrt3*, the earliest and predominant family member is activated at E6.5 in the extra-embryonic anterior visceral endoderm (AVE). *Flrt2* is weakly co-expressed in the AVE, but with a delayed onset beginning at

[1]The Sir William Dunn School of Pathology, University of Oxford, South Parks Road, Oxford OX1 3RE, UK. [2]Department of Physiology, Anatomy and Genetics, University of Oxford, South Parks Road, Oxford OX1 3RE, UK.

*Present address: Department of Molecular Oncology, Goettingen Center of Molecular Biosciences, GZMB, University of Goettingen, Justus von Liebig Weg 11, D-37077 Goettingen, Germany
†Present address: Centre for Chromosome Research, Department of Biochemistry, NUI Galway, Distillery Road, Galway, Ireland
‡Author for correspondence (elizabeth.robertson@path.ox.ac.uk)

Accepted 6 January 2011

E7.5 (Maretto et al., 2008). One day later, *Flrt2* shows very strong expression in the trunk mesenchyme beneath the forming heart (Maretto et al., 2008). By E10.5, *Flrt2* and *Flrt3* expression domains broadly overlap within the pharyngeal mesenchyme, developing heart, somites and central nervous system (CNS) (Haines et al., 2006; Maretto et al., 2008). By contrast, *Flrt1* expression is restricted to the developing brain.

In *Xenopus*, Flrt3 guides cell movements, regulates cell de-adhesion and modulates Fgf signalling at gastrulation stages (Bottcher et al., 2004; Ogata et al., 2007). In mouse embryos, Flrt3 is required to maintain tissue integrity and organize the underlying basement membrane (BM) in the AVE signalling centre that governs establishment of the anterior-posterior body axis (Egea et al., 2008; Maretto et al., 2008). *Flrt3*-deficient embryos gastrulate abnormally and nearly all die by E10.5, displaying a spectrum of tissue disturbances that include defective head fold fusion, definitive endoderm migration and ventral closure failure, which leads to cardia bifida (Egea et al., 2008; Maretto et al., 2008).

Here, we describe partially overlapping *Flrt2* and *Flrt3* expression domains in the developing heart. Interestingly, *Flrt2* and *Flrt3* are both strongly expressed in the PEO. However, *Flrt3* is selectively downregulated following attachment and outgrowth of the epicardial cells, and beginning at around E10 only *Flrt2* expression is maintained in the fully delaminated epicardium. By contrast, *Flrt2* and *Flrt3* co-expression is maintained throughout the myocardium until around E12.5.

To investigate *Flrt2* functional activities in vivo, we generated a null allele via gene targeting. Nearly all homozygous mutant embryos arrest at mid-gestation (E12.5) owing to cardiac insufficiency. Consistent with its unique expression domain, *Flrt2*-deficient hearts display defects in the integrity of the epicardium and disturbances to the architecture of the underlying BM accompanied by a pronounced reduction in thickness of the ventricular myocardium. As for the *Flrt3* mutant AVE, we also observe here disruptions in the epicardial cell layer, suggesting that Flrt2 and Flrt3 might contribute similar functional activities in the epicardium and AVE, respectively. To test this possibility, we exploited in vitro and in vivo reconstitution assays. Interestingly, *Flrt2* expression efficiently corrects the abnormal morphology and disorganized BM phenotype of *Flrt3* mutant embryoid bodies (EBs), and similarly ectopic *Flrt3* expression in the epicardium of *Flrt2* null embryos rescues heart development. The present results demonstrate that either Flrt2 or Flrt3 expression alone is sufficient to maintain tissue integrity within the AVE or the epicardium. Consistent with previous reports (Egea et al., 2008; Maretto et al., 2008), we also demonstrate here, as for *Flrt3*, that *Flrt2* expression is independent of Fgf signalling.

MATERIALS AND METHODS

Mouse strains and genotyping

The *Flrt2*-null allele was generated by replacing a 2.9 kb region encompassing the entire coding exon with a *loxP*-flanked PGK-*hygromycin* resistance cassette. The flanking genomic regions comprised of the 3 kb 5′ (*Eco*RV-*Eco*RV) and 5.7 kb 3′ (*Sma*I-*Sma*I) arms isolated by PCR (Expand Long Template PCR System, Roche Applied Science, Basel, Switzerland), were subcloned into *Swa*I and *Pme*I sites present in the *LoxP-flanked pgk-hygro*-containing vector, flanked with hsv-tk- and pgk-DTA-negative selection cassettes, as described previously (Vincent et al., 2004). The *Not*I linearized vector was electroporated into CCE ES cells. DNA from drug-resistant colonies was digested with *Stu*I and screened by Southern blot hybridization with a 5′ external probe and subsequently re-screened with an internal *hygro* probe. From 960 drug-resistant colonies, we recovered two correctly targeted clones that were injected into C57BL/6J blastocysts to generate germ line chimeras. The mutation was maintained on a 129/C57Bl/6J genetic background.

Genotyping by PCR

The following three primers were used: F2-4FW, 5′-CTGCCACATCCC-CAACAACATGAGAT; F2-5RV, 5′-TCAACAGCGAAGTGGTTAATC-TGCATC; and HYG-FW, 5′-TTTGAATGGAAGGATTGGAGCTACG-GGG. After 36 cycles of 94°C for 45 seconds, 64°C for 1 minute, a 72°C extension for 1 minute and a final extension at 72°C for 10 minutes, 419 bp (wild type) and 500 bp (mutant) products were resolved on a 2% agarose gel.

To generate transgenic constructs full-length *Flrt2* or *HA-Flrt3* cDNAs (Maretto et al., 2008) were subcloned into the pCAGGs expression vector (Niwa et al., 1991; Dunn et al., 2005). The expression cassettes comprising a CAG promoter with either *Flrt2*- or *HAFlrt3*-coding information followed by the rabbit β-globin pA were excised and injected into fertilized $(C57CBA)F_1$ oocytes. Transgene-positive founder animals were identified by PCR with primers specific for the unique pCAGG intronic sequence: FW, 5′-CCTTTTATGGTAATCGTGCGAG-3′; RV, 5′-CGAGGCTGGAG-ATGGAGAAG-3′.

After 36 cycles of 94°C for 30 seconds, 60°C for 30 seconds, 72°C for 1 minute and a final extension at 72°C for 5 minutes, the 195 bp product was detectable on a 2% agarose gel. Founder animals were confirmed by Southern blot hybridization using *Nde*I-digested DNA with an internal probe derived from either the *Flrt2*- or *Flrt3*-coding exon. *TgFlrt2* and *tgHAFlrt3* expression was subsequently tested by RT-PCR and western blot analysis on adult tissues taken from representative transgenic offspring. *tgHAFlrt3* and *tgFlrt2* transgenic mice were then crossed to *Flrt3* (Maretto et al., 2008) or *Flrt2* heterozygous animals carrying the null alleles. Transgene positive heterozygous offspring were subsequently backcrossed to *Flrt2* or *Flrt3* heterozygotes to evaluate possible rescue of the embryonic lethalities.

Cell lines

Cos7 cells were transfected using Lipofectamine2000 (Invitrogen, Carlsbad, CA, USA) according to the manufacturer's guidelines. *Flrt3* homozygous mutant ES cell lines were isolated from blastocysts from *Flrt3* heterozygous intercrosses as described (Robertson, 1987), and genotyped by Southern blot analysis (Maretto et al., 2008). *Flrt3* mutant ES cell lines were transfected with linearized pCAGG *Flrt2* and *HAFlrt3* expression vectors, and drug resistant colonies screened by Southern blot analysis were subsequently tested for protein expression by western analysis. Embryoid bodies were generated using standard protocols (Robertson, 1987). The LyEnd.1 endothelial cell line (a kind gift from Dr Friedemann Kiefer, Münster, Germany) was grown as described (Ong et al., 2001).

Production of Flrt2 antibodies and western blots

The region encoding the Flrt2 extracellular domain corresponding to amino acids 1-525 was cloned in-frame into *Eco*RI and *Kpn*I sites of the pHLsec expression vector containing the hexahistidine (His6) tag (Aricescu et al., 2006a). Numbering corresponds to GenBank entry NP_848469. C-terminally His6-tagged Flrt2 protein produced by transiently transfected HEK 293 cells and purified as described previously (Aricescu et al., 2006b; Maretto et al., 2008) was injected into rabbits. Cell lysates were prepared as described previously (Koonce and Bikoff, 2004). Proteins resolved by SDS-PAGE were transferred onto PVDF membranes (Millipore, Billerica, MA, USA). Blots were probed with F2-HIS, F3-cyt (Ogata et al., 2007) rabbit polyclonal antibodies, Erk (Cell Signaling, Danvers, MA, USA; 4695, 1:1000), pErk (Cell Signaling, 9101, 1:1000) or HA (Roche 1867431, 1:2500) antibodies followed by HRP-conjugated secondary antibodies (Jackson ImmunoResearch, West Grove, PA, USA) and developed by chemiluminescence using ECL (Amersham Bioscience Europe, Piscataway, NJ, USA).

In situ hybridization, X-gal staining, immunohistochemistry and scanning electron microscopy

In situ hybridization on intact embryos and paraffin sections were performed according to standard protocols (Nagy, 2003) using the following probes: *Flrt2*, *Flrt3* (Maretto et al., 2008), *Tbx18* (Kraus et al., 2001), *Wt1* (Armstrong et al., 1993) and *Tbx20* (Carson et al., 2000). *lacZ*

activity was visualized by whole-mount X-gal staining as described (Nagy, 2003). Haematoxylin and Eosin staining was performed according to standard protocols.

For immunohistochemistry, embryos were fixed overnight in 4% PFA, dehydrated through an ethanol series, embedded in paraffin wax and sectioned at 7 μm. Sections were subjected to antigen retrieval by boiling for 20 minutes in 10% Target Retrieval Solution (DAKO 51699, Carpinteria, CA, USA), blocked for 5 minutes in peroxidase block (DAKO K4011), washed in PBS-Tween-20 and incubated overnight at 4°C in primary antibody αSMA (1:500; M0851; DAKO), αKi-67 (1:200; NCL-L-Ki67-MM1; Novocastra Laboratories, Newcastle upon Tyne, UK), αF2-HIS, αF3-Cyt, re-washed in PBS-Tween-20 and then developed using the appropriate DAKO peroxidase-labelled polymer kit and DAB, then counterstained with Haematoxylin.

For IHC on cryosections, embryos and hearts were fixed for 2 hours in 4% PFA and equilibrated in 9% sucrose then 18% sucrose overnight at 4°C before transferring into OCT and freezing in isopentane on dry ice. Sections (8 μm) were cut and post-fixed in acetone, blocked with 10% goat serum/1% bovine serum albumin/PBS for 1 hour. Embryoid bodies (EBs) were harvested at day 5 of differentiation and fixed for 30 minutes in 4% PFA. EBs were equilibrated with 7.5% sucrose, then 15% sucrose overnight at 4°C. Samples were then frozen and processed as above. Sections were permeabilized with methanol for 10 minutes at –20°C and blocked with 10% goat serum/1% bovine serum albumin/PBS for 1 hour. The following primary antibodies: VCAM-1 (BD Pharmingen, Oxford, UK; 1:100), α4β1 integrin (BD Pharmingen, 1:100), F2-HIS (1:1000), αF3-cyt (1:2000), laminin (Sigma, St Louis, MO, USA; L-9393, 1:400) and collagen IV (Chemicon, Billerica, MA, USA; AB756, 1:100) were detected with AlexaFluor-conjugated secondary antibodies (Molecular Probes, Carlsbad, CA, USA).

For whole-mount staining, hearts were dissected in ice-cold PBS, fixed in 4% PFA for 2 hours at 4°C, dehydrated in methanol, bleached with 5% H_2O_2, rehydrated, blocked with 3% non-fat milk/0.1% Triton X-100/PBS (PBSMT), incubated with primary antibody overnight (α-mouse CD31, BD Pharmingen 550274, 1:150 in PBSMT; α-HA Roche 1867431, 1:1000 in PBSMT), washed extensively, incubated with secondary antibody overnight and washed extensively. The colour was developed using DAB.

For scanning electron microscopy (SEM) embryos were dissected in DMEM plus 10% FCS, fixed overnight (2.5% glutaraldehyde, 2% paraformaldehyde, 0.1% picric acid in 100 mN phosphate buffer at pH 7.0), post-fixed for 1.5 hours in 1% osmium/100 mM phosphate buffer (pH 7.0) and subsequently processed according to standard protocols. Images were taken on a JEOL JSM 6390 SEM.

Morphometric analysis

Myocardial and endocardial morphometric analyses were conducted using ImageJ software. SMA- or Flk1-positively stained areas were automatically selected using the software and the number of pixels highlighted

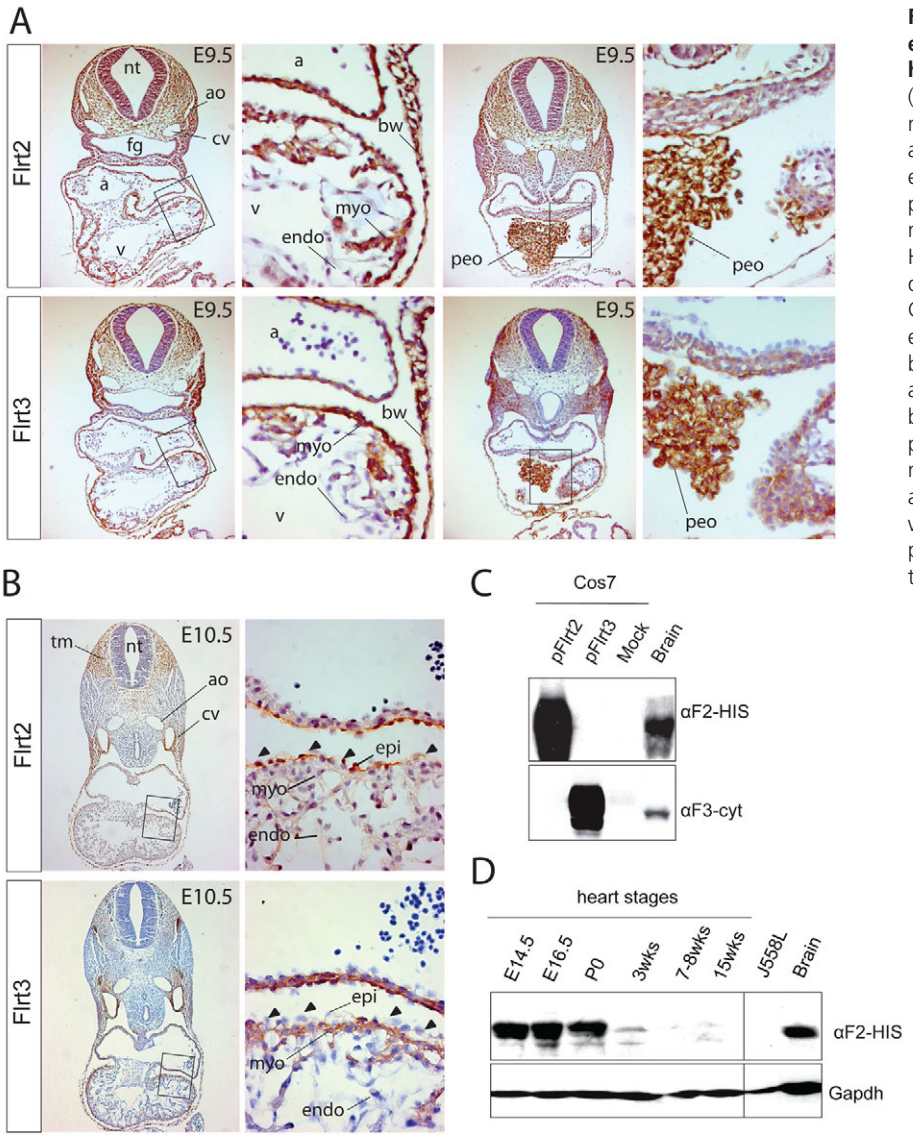

Fig. 1. Developmentally regulated expression of Flrt2 and Flrt3 proteins in the heart. (A,B) Immunohistochemistry on sections. (**A**) Flrt2 and Flrt3 proteins are localized in the myocardium, body wall and pro-epicardial organ at E9.5. (**B**) At E10.5, Flrt2 but not Flrt3 is expressed in the epicardial cell layer. Both proteins are expressed throughout the myocardium. (**C**) Western blot showing that F2-HIS and F3Cyt (Ogata et al., 2007) specifically detect Flrt2 and Flrt3 proteins in transfected Cos7 cell lysates. Both antibodies react against endogenously expressed Flrt proteins in the adult brain. (**D**) Western blot analysis shows Flrt2 is abundantly expressed in developing heart tissue, but expression levels decline postnatally. J558L plasmacytoma cells served as a negative control. nt, neural tube; ao, aorta; cv, cardinal vein; a, atrium; v, ventricle; fg, foregut pocket; bw, body wall; myo, myocardium; endo, endocardium; peo, pro-epicardium/pro-epicardial organ; tm, trunk mesenchyme; epi, epicardium.

corresponded specifically to the stained area of the image. Statistical analysis was performed using the Prism5 statistic software and Student's *t*-test.

Imaging epicardial explants and whole-mount hearts

E10.5 and E11.5 hearts harvested in 1×Hanks-buffered salt solution, were placed dorsal side downwards on collagen-coated slides (BD Biosciences) and cultured for up to 72 hours in M119 medium containing 5% foetal calf serum (Austin et al., 2008). The outgrowths were fixed in 4% PFA/PBS for 10 minutes and permeabilized with 0.2% TritonX-100 for 5 minutes at room temperature, then blocked in 10% goat serum/1% BSA/PBS for 1 hour at room temperature. Tissue was stained with ZO-1 (Invitrogen, 40-2200, 1:400) and Phalloidin (Molecular Probes, A22284, 1:40), washed and incubated in secondary antibody for 1 hour at room temperature, then washed and mounted in Vectashield +DAPI (Vector Laboratories, H-1200).

For whole-mount immunofluorescence, hearts were isolated at E10.5 and E11.5 in ice-cold PBS, fixed in 4% PFA for 15 minutes. Samples were washed in PBS-Triton-X100 before permeabilization and blocking (PBS/0.1% Triton-X100, 0.2%BSA, 5% FCS), and washed again before the addition of primary antibodies overnight at 4°C: 1:200 Perlecan (Millipore, MAB1948), 1:500 ZO-1 (Invitrogen, 40-2200), 1:40 Phalloidin (Molecular Probes). Following extensive washing in PBS/0.1% Tween-20, hearts were incubated with AlexaFluor-conjugated secondary antibodies (Molecular Probes) overnight at 4°C, then washed again in PBS/0.1% Tween-20 and 1:1000 DAPI (Sigma) for 20 minutes before re-washing and mounting in Vectashield (Vector Laboratories). Hearts were imaged by confocal microscopy using a Zeiss LSM 710.

Fgfr1 inhibition explant cultures

E11.5 hearts harvested in 1×Hanks buffered salt solution were cultured for 24 hours at 37°C, 5% CO_2 in M199 containing 5% foetal calf serum and 40 μM SU5402 (Calbiochem, Gibbstown, NJ, USA), or DMSO alone. RNA was extracted using the RNeasy Mini Kit (Qiagen, Valencia, CA, USA; 74104), and tissue homogenized with QIAshredde (Qiagen, 79654) according to the manufacturer's instructions. Total RNA (50 ng) was analysed using the QIAGEN One-Step RT-PCR kit (210212; Qiagen). Reverse transcription was performed by incubating at 50°C for 30 minutes, followed by heat inactivation at 95°C for 15 minutes then 94°C for 30 seconds, annealing at optimised temperature for 30 seconds and extension at 72°C for 30 seconds, with a final extension step at 72°C for 5 minutes. Cycling conditions were optimized according to the primer pair and the amount of product amplified. The following primer sets were used: Flrt2 1FW, 5′-GATTCGGATGAGCTAAGGAG-3′ and Flrt2-1RV, 5′-TTTGAGGATGAAAGCCCCAC-3′ for 36 cycles at 58°C; Flrt3-2F, 5′-GGGGGAGGGTTTTTACTTCAACTC-3′ and Flrt3-2RV, 5′-AACT-GACAGAGGTGCCACTTGG-3′ for 27 cycles at 58°C; Hprt-F1, 5′-GCTGGTGAAAAGGACCTCT-3′ and Hprt-F2, 5′-CACAGGACTA-GAACACCTGC-3′ for 27 cycles at 58°C.

RESULTS

Partially overlapping Flrt2 and Flrt3 expression domains in the developing heart

Dynamic *Flrt1*, *Flrt2* and *Flrt3* expression patterns between E6.5 and E10.5 of mouse development have been previously documented (Haines et al., 2006; Maretto et al., 2008). *Flrt3* transcripts are strongly and broadly expressed beginning at earliest post-implantation stages; *Flrt2* expression shows a more restricted pattern of expression; and *Flrt1* expression is largely confined to the developing CNS. To extend these observations here, we examined expression in the developing heart using Flrt2- and Flrt3-specific rabbit antibodies. At E8.5, coincident with formation of the looping heart tube, Flrt2 is strongly expressed in the myocardial layer, but absent from the inner endocardial cell population. By contrast only low levels of Flrt3 are detectable in the myocardium (see Fig. S1 in the supplementary material). The PEO, which is induced immediately ventral to the inflow tract of the heart, first becomes visible at E8.5-E9.0 as two loose clusters of cells on either side of the midline, that express characteristic markers such as *Wt1* (Armstrong et al., 1993) and *Tbx18* (Kraus et al., 2001). At E9.5, PEO cells that have migrated to the midline strongly express both Flrt2 and Flrt3 (Fig. 1A). However, 24 hours later, following attachment and migration of the epicardial cell aggregates onto the dorsal surface of the heart, Flrt3 expression is markedly downregulated. By contrast Flrt2 expression is robustly maintained throughout the entire sheet of epicardium (Fig. 1B). Similarly, at E9.5 and E10.5, Flrt2 and Frlt3 are co-expressed in the atrial myocardial layer and compact ventricular myocardium, but by E14.5 Flrt3 expression becomes almost completely restricted to the

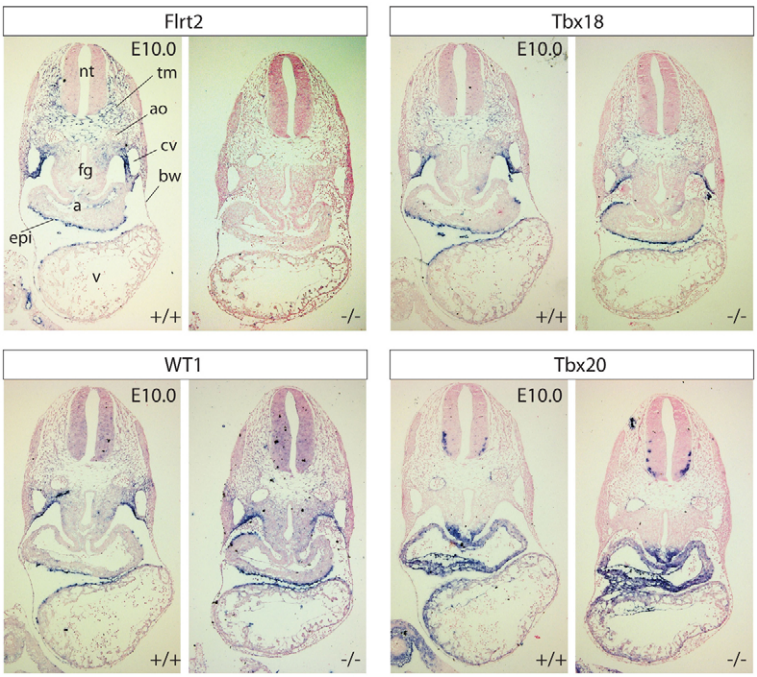

Fig. 2. *Flrt2*-null embryos correctly specify the pro-epicardial organ. In situ hybridisation on sections with Eosin counterstaining. The epicardium forms normally in *Flrt2*-null embryos, as judged by expression of *Tbx18* and *Wt1* at E10.0. Similarly, expression of *Tbx20* demonstrates correct specification of anterior heart field derivatives in the mutants. nt, neural tube; ao, aorta; cv, cardinal vein; a, atrium; v, ventricle; fg, foregut pocket; bw, body wall; tm, trunk mesenchyme; epi, epicardium.

DEVELOPMENT

neural tube (see Fig. S1 in the supplementary material). Western blot analysis (Fig. 1D) and immunohistochemical experiments (see Fig. S1 in the supplementary material) demonstrate that Flrt2 expression persists in the heart throughout embryogenesis, but declines postnatally.

Flrt2-deficient embryos arrest at midgestation due to cardiac insufficiency

To investigate *Flrt2* requirements in vivo, we engineered a null allele by replacing the single coding exon (exon 2) with a loxP flanked drug resistance cassette (see Fig. S2 in the supplementary material). Two independent correctly targeted ES cell clones were used to generate germline chimeras. Heterozygous offspring were healthy and fertile, and homozygous mutant embryos were recovered from intercross matings at the expected Mendelian ratios at early stages (Table 1). However, the majority of *Flrt2* mutant embryos die between E11.5 and E12.5. As for *Flrt3* mutants (Egea et al., 2008; Maretto et al., 2008), a small fraction (3%) complete development and are viable and fertile as adults. Western blot experiments confirmed the mutation eliminates *Flrt2* expression (see Fig. S2D in the supplementary material).

Midgestation lethality is usually caused by placental or cardiovascular defects. *Flrt2*-deficient embryos were readily identified at E11.5/E12.5 due to blood pooling, superficial haemorrhaging and pericardial oedema but were otherwise indistinguishable from littermates (data not shown). *Flrt2* expression in the placenta is restricted to the endothelium of the foetal blood vessels (data not shown). An extensive histological analysis failed to demonstrate any placental abnormalities (see Fig. S3A in the supplementary material). Importantly, at E10.5 and E11.5 the labyrinth region, the site of foetal maternal exchange, forms normally. Additionally, when the integrity and organization of the placental foetal blood vessels was examined using *Flk1.lacZ* and *Flt1.lacZ* endothelial-specific reporter genes (Shalaby et al., 1995; Fong et al., 1995), the patterns of *lacZ* staining observed in wild-type and *Flrt2* mutants were indistinguishable (see Fig. S3B in the supplementary material).

Flrt2 is also strongly expressed in the mesenchyme surrounding the major thoracic blood vessels at E9.5 and 10.5 (Fig. 1A,B). Thus, another possibility is that loss of Flrt2 potentially causes the vessel wall to become fragile and rupture coincident with increased haemodynamic pressure at midgestation. However, careful analysis of $Flrt2^{-/-}$*:Flk1.lacZ* embryos (n=10) failed to reveal any damage or patterning defects within the major blood vessels (data not shown).

Xenopus Flrt3 and zebrafish Flrt3, Flrt1a and Flrt1b proteins have been shown to interact with Unc5b, a homologue of the netrin receptor (Chen et al., 2009; Karaulanov et al., 2009; Sollner and Wright, 2009). Mouse embryos lacking *Unc5b* die at around E12.5 due to excessive sprouting within the peripheral capillary network that secondarily causes collapse of the arterial vessels (Lu et al., 2004). To test for possible defects in the peripheral vasculature, we examined the capillary networks in the developing fore- and hindbrains of E10.5 wild-type and mutant *Flk1.lacZ*-stained embryos. There were no noticeable differences in the number and patterning of superficial capillaries (see Fig. S4 in the supplementary material). Rapid growth of the heart depends on the development of the coronary vasculature. Starting at E11.5, angiogenic sprouts originating from the sinus venosus migrate into the myocardium located in the dorsal interventricular region to form the initial vascular plexus, which then undergoes reprogramming to form the coronary vessels (Red-Horse et al., 2010). To examine possible defects in formation of the coronary vasculature, we performed whole-mount Pecam1 staining of wild-type and *Flrt2* mutant hearts at E11.5. We found no visible differences in the architecture or density of the nascent coronary vascular plexus (see Fig. S4 in the supplementary material). Thus, we conclude that developmental arrest of *Flrt2* mutant embryos at midgestation cannot be explained by placental or vascular defects.

Mutant hearts also showed normal patterns of marker gene expression at E10.0 (Fig. 2; data not shown). As judged by *Tbx18* and *Wt1* expression, the epicardial cells attach and migrate on the dorsal wall of the heart with normal kinetics. Similarly, *Tbx20* expression essential for expansion of cardiac progenitors and myocardial specification (Stennard et al., 2005) is unperturbed (Fig. 2).

At E11.5, proliferation of the outermost myocytes in response to trophic signals from the overlying epicardium promotes rapid expansion of the ventricular compact zone (for a review, see Lavine and Ornitz, 2009). Differentiation of the inner myocardial layer results in the formation of bundles of finger-like trabeculated cardiomyocytes covered in a monolayer of endocardium. These developmental changes prior to E12.5 are essential to increase the myocardial surface, enhance contractility and ensure directional pumping of the oxygenated blood prior to completion of chamber septation and formation of the endocardial cushions (for a review, see Sucov, 1998). To assess development of the myocardium and endocardium, we examined smooth muscle actin and *Flk1.lacZ* staining, respectively (Fig. 3). Interestingly, *Flrt2* loss of function results in a significant decrease in thickness of the compact zone, accompanied by a concomitant decrease in volume of the *Flk1.lacZ*-positive endocardium (Fig. 3A-D). To investigate potential changes in mitotic activity, we compared the percentage of proliferating cells in wild type versus mutant. However, there were no significant differences in Ki67 immunostaining (see Fig. S5 in the supplementary material). Overall, *Flrt2* mutant hearts

Table 1. Genotyping results from Flrt2 heterozygous intercross matings

	Genotype			
Age	+/+	+/–	–/–	Total
9.5 dpc	21 (25.0%)	42 (50.0%)	21 (25.0%)	84
10.5 dpc	36 (19.6%)	108 (58.7%)	40 (21.7%)	184
11.5 dpc	161 (25.0%)	314 (50.0%)	161 (25.0%)	636
12.5 dpc	25 (27.2%)	56 (60.9%)	12 (13.0%)*	93
15.5 dpc	16 (34.8%)	26 (56.5%)	4 (8.7%)*	46
17.5 dpc	10 (43.5%)	12 (52.2%)	1 (4.3%)	23
Weanlings	219 (38.2%)	339 (59.2%)	15 (2.6%)	573

The table shows total numbers and corresponding percentages of embryos recovered at the indicated stages and weanlings from *Flrt2* intercross matings.
*75% of mutant embryos recovered at E12.5 and E15.5 were necrotic.

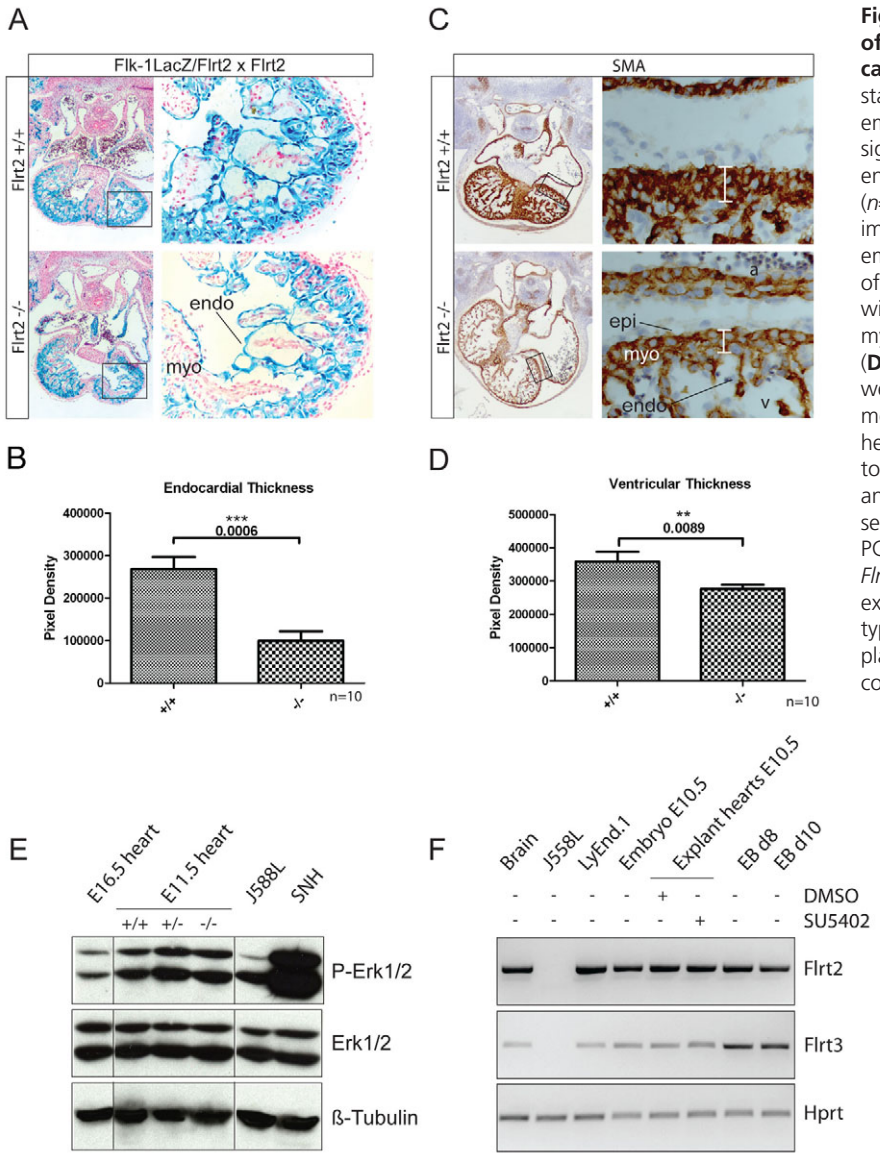

Fig. 3. Loss of Flrt2 results in impaired expansion of the compact ventricular myocardium and causes a reduction in endocardial volume. (**A**) *lacZ* staining (blue) of *Flrt2:Flk-1.lacZ*-null and wild-type embryos at E11.5. (**B**) Image J analysis shows a significant (P=0.0006) reduction in the volume of the endocardium lining the inner surface of the heart (n=10). Data are mean±s.e.m. (**C**) SMA immunohistochemical staining of E11.5 Flrt2-deficient embryos shows a significant reduction in the thickness of the compact ventricular myocardium compared with wild-type littermates. a, atrium; v, ventricle; myo, myocardium; endo, endocardium; epi, epicardium. (**D**) Differences in myocardial thickness (P=0.0089) were quantitated using Image J (n=10). Data are mean±s.e.m. (**E**) Western blot analysis of total E11.5 heart lysates shows no differences in the expression of total ERK and phospho-ERK levels between wild-type and mutant embryos. SNH embryonic fibroblasts served as a positive control. (**F**) Semi-quantitative RT-PCR analysis shows equivalent expression of *Flrt2* and *Flrt3* mRNA in control and SU5402-treated heart explants. Lanes contain RNA from adult brain, wild-type d8 and d10 embryoid bodies. LyEnd.1 and J558L plasmacytoma cells served as a positive and negative controls, respectively.

have relatively thin ventricular walls, markedly reduced trabeculae and appear dilated in comparison with littermate controls. These findings strongly suggest that *Flrt2* mutant embryos die at E12.5 because of cardiac insufficiency.

The Fgf signalling pathway contributes to expansion of the compact cardiomyocyte layer (Lavine et al., 2005), and experiments in *Xenopus* and transfected cell lines suggest Flrt proteins modulate the strength of Fgf signalling via a regulatory feedback loop (Bottcher et al., 2004; Haines et al., 2006). To assess Fgf signalling activity in *Flrt2* mutant hearts, we examined phospho-Erk1/2 levels using western blot analysis. As shown in Fig. 3E, phospho-Erk1/2 levels were unperturbed in the absence of *Flrt2* expression. Additionally, to test whether Fgf signalling regulates *Flrt2* expression, we treated E7.5 embryos and E10.5 heart explant cultures overnight in the presence of the FgfR1 inhibitor SU5402, as described previously (Maretto et al., 2008). As assessed by either semi-quantitative RT-PCR or whole-mount in situ hybridization analysis (Fig. 3F; data not shown) there was no noticeable change in *Flrt2* expression levels. Furthermore, histological analysis of control, without SU5402, versus treated hearts failed to reveal morphological differences (see Fig. S6 in the supplementary material). As for *Flrt3* (Egea et al., 2008; Maretto et al., 2008), *Flrt2* expression also appears to be independent of Fgf signalling.

Flrt2 functions in the epicardium to maintain tissue integrity and organize components of the basement membrane

Mutations that disrupt the association of the epicardium with the underlying myocardium, i.e. loss of α4β1-integrin or its cognate receptor Vcam1, result in decreased thickness of the myocardium (Kwee et al., 1995; Yang et al., 1995; Sengbusch et al., 2002). To test the possibility that *Flrt2* functional loss disrupts expression of α4β1-integrin in the epicardium and/or Vcam1 in the basal cardiomyocytes, we performed immunostaining experiments. As shown in Fig. 4, loss of Flrt2 has no noticeable effect on either Vcam1 or α4β1-integrin expression.

To further investigate tissue disturbances in the mutant epicardium, we performed SEM on intact E11.5 hearts. As expected, the wild-type epicardial sheet has a flattened cobblestone-like appearance (Fig. 5A). In striking contrast, the

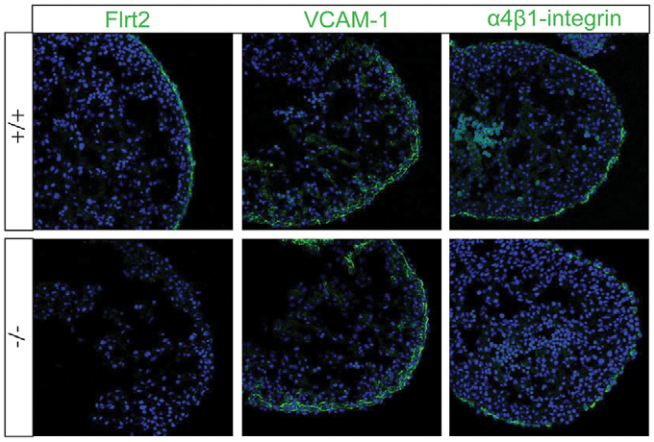

Fig. 4. Loss of Flrt2 does not affect the expression of Vcam1 or α4β1-integrin in the heart. Vcam1 and α4β1-integrin staining in cryosections of E10.5 *Flrt2* mutant and wild-type heart tissues shows that both are efficiently expressed in the *Flrt2*-deficient hearts (*n*=2).

mutant epicardium appears ruffled and uneven. Moreover at high magnification, we observed numerous holes in the surface that expose the underlying fibrous ECM associated with the sub-epicardial space. These perforations closely resemble those recently described in *Flrt3* mutant visceral endoderm (Egea et al., 2008).

Next, we examined explant cultures from intact E11.5 hearts. Epicardial cells were allowed to migrate from the surface of the heart onto a collagen-coated substrate (Austin et al., 2008). The resulting monolayers were stained with antibodies directed against ZO-1 and phalloidin to visualize the plasma membrane and actin cytoskeleton architecture, respectively (Fig. 5B). Consistent with results above, the wild-type epicardium forms a coherent sheet of tightly opposed cells. In striking contrast, the *Flrt2* mutant epicardium displays numerous discontinuities disrupting cell-cell contacts. Unlike the wild-type epicardium that is tightly attached to the underlying myocardium and separated by a thin uniform layer of BM, confocal images of ZO-1/phalloidin double stained *Flrt2* mutant hearts show the surface of the epicardial layer is highly uneven (Fig. 6A). Additionally, mutant hearts display localized Perlecan depositions and an overall increase in the thickness of the BM layer (Fig. 6B). Thus, as for *Flrt3* mutant visceral endoderm (Egea et al., 2008), loss of *Flrt2* disrupts tissue integrity and BM architecture in the epicardium.

Functionally interchangeable roles shared by closely related Flrt3 and Flrt2

Flrt3 and Flrt2 family members share 45% amino acid sequence identity (Lacy et al., 1999) and display similar activities in gain-of-function assays. For example, both Xflrt2 and Xflrt3 mediate homotypic interactions and drive cell sorting in transiently transfected mammalian cells (Karaulanov et al., 2006). Our results

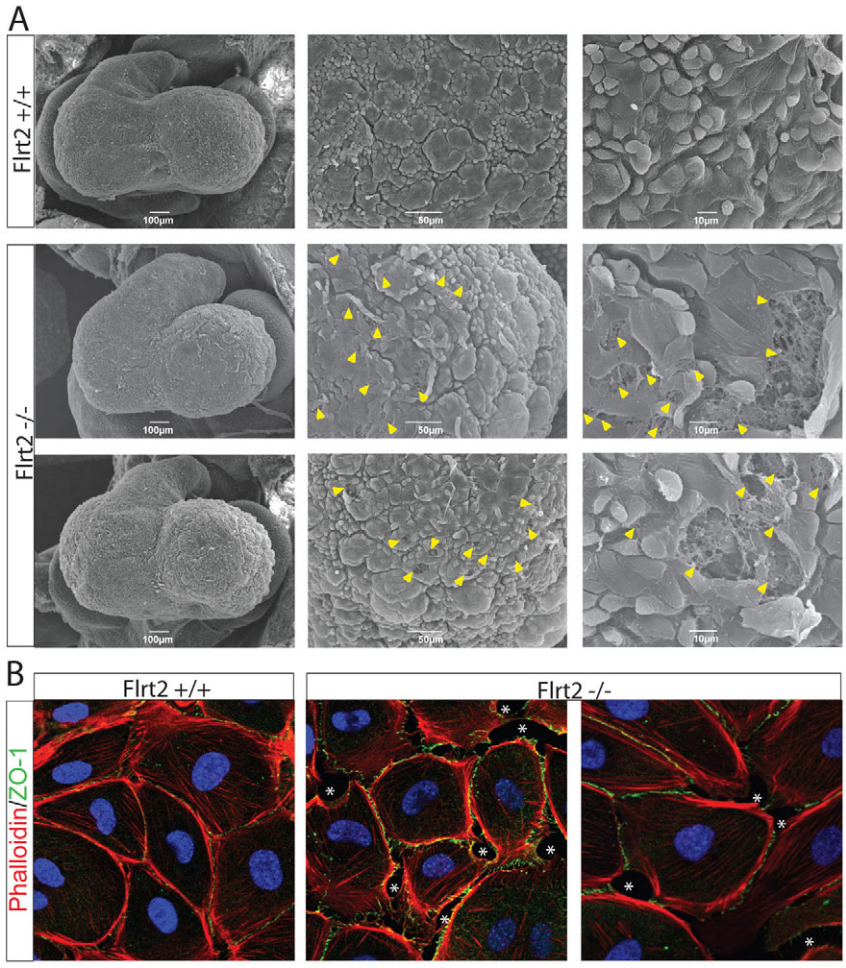

Fig. 5. Loss of *Flrt2* compromises epicardial integrity. (**A**) SEM analysis of the ventral surface of E11.5 hearts reveals numerous disruptions to the epicardial cell layer on the surface of *Flrt2* mutants compared with wild-type littermates (*n*=10). (**B**) E11.5 epicardial explant cultures immunostained with ZO-1 antibody (green) and phalloidin (red) show many discontinuities and areas of loss of cell contact in the Flrt2 outgrowths (white asterisks) compared with wild-type cultures (*n*=10).

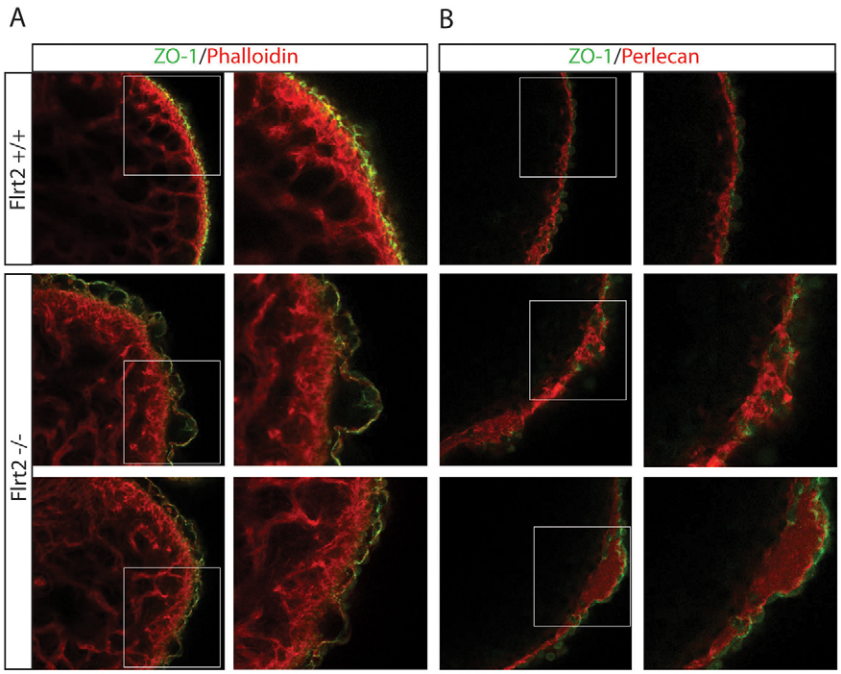

Fig. 6. Whole-mount analysis of *Flrt2* mutant hearts demonstrates detachment of the epicardial layer and disruption of the basement membrane. (**A**) At E10.5, ZO-1 staining (green) shows the epicardium is normally tightly opposed to the myocardium, but in *Flrt2*-null embryos many areas of epicardial cell detachment from the underlying sub-epicardial serosa can be seen (*n*=5). (**B**) Staining for the basement membrane (BM) marker perlecan clearly demonstrates disorganization and local accumulations of BM between the epicardium and myocardium in mutant hearts.

presented above strongly suggest that Flrt2 and Flrt3 play conserved functional roles in maintaining cell-cell contacts in the epicardium and AVE, respectively.

To assess functional redundancy directly, we initially examined the ability of Flrt2 activity to rescue tissue disturbances in the context of *Flrt3* mutant EBs. Flrt3 is strongly expressed in the primitive endoderm layer that forms on the surface of EBs (Fig. 7). The *Flrt3* mutant EBs display a characteristic BM disorganization and develop distinctive protrusions (Egea et al., 2008) (Fig. 7C,D). We decided to test whether *Flrt2* and, as a control, HA-tagged *Flrt3* expressed under control of the CAGGS promoter, could rescue these defects. A panel of stably transfected *Flrt3* mutant ES cells transfected with either *Flrt2* or *HA-Flrt3* expression constructs was screened by western blot analysis. Two independent clones expressing each construct were used to generate EBs and the reconstituted EBs were stained for collagen IV and laminin to visualize BM components. As expected, *HA-Flrt3* efficiently rescues BM disorganization and morphological defects (Fig. 7C,E). Interestingly, *Flrt2* functions equally well in this context to reconstitute *Flrt3*-deficient EBs.

Next, to evaluate *Flrt2* and *Flrt3* shared activities in vivo, we used these expression constructs to generate transgenic mice. The progeny of transgenic founders were screened by western blot analysis to identify lines that ectopically express the transgenes throughout adult somatic tissues (data not shown). Transgene expression at early stages of embryonic development was also examined. In contrast to endogenous *Flrt2*, which is only weakly expressed within the AVE at E7.0 (Fig. 8A), tg*Flrt2* is readily detectable throughout the epiblast and overlying VE. At E10.5, *Flrt3* expression is normally confined to the myocardium (Maretto et al., 2008) (Fig. 8B). We were able to identify a tg*Flrt3* transgenic line that is strongly expressed in the epicardium, but not the underlying myocardium (Fig. 8B). The tg*Flrt2* and tg*HA-Flrt3* strains were then crossed to *Flrt3* or *Flrt2* heterozygous mutant partners, respectively. Transgene positive heterozygous offspring were intercrossed and the resulting weanlings genotyped. In both cases, we found more that 50% of the transgene positive homozygous mutant embryos are rescued and viable postnatally (Table 2). Thus, 17% of the tg*Flrt2* animals (*n*=87) were homozygous *Flrt3* mutants. These results demonstrate that ectopic *Flrt2* expression in the AVE can rescue the gastrulation defects. Similarly, 13% of the tg*HAFlrt3* animals (*n*=69) proved to be *Flrt2* mutants. ZO-1 staining of E11.5 explant cultures confirmed that ectopic *Flrt3* expression restores epicardial integrity (see Fig. S7 in the supplementary material). Thus, *Flrt3* expression in the epicardium partially substitutes for loss of *Flrt2*. Collectively, these results demonstrate that closely related *Flrt2* and *Flrt3* family members share similar functional roles in the developing mouse embryo. The null phenotypes are associated with an inability to maintain tissue integrity at unique expression sites.

DISCUSSION

Three closely related Flrt1-Flrt3 family members, conserved across vertebrate evolution, all share key structural features: 10 leucine-rich repeats flanked by cysteine-rich regions, a type III fibronectin domain followed by the transmembrane segment and a short intracellular tail (Lacy et al., 1999). As for other LRR cell-surface molecules, including Toll-TLR receptors, the extracellular LRR domain probably forms a characteristic ‘horseshoe’-shaped structure that mediates a wide range of recognition processes (for a review, see Bell et al., 2003; Kobe and Kajava, 2001). Recent evidence suggests that associations between *Xenopus* Flrt3 or zebrafish Flrt3, Flrt1a and Flrt1b LRR modules, and the Unc5b ectodomain control cell-cell interactions in the developing embryo (Karaulanov et al., 2009; Sollner and Wright, 2009). Interestingly, zebrafish Flrt3, Flrt1a and Flrt1b display a surprising degree of quantitative variation in receptor-binding strength (Sollner and Wright, 2009). Phosphorylation of the Flrt1 cytoplasmic tail has been shown to modulate MAPK activity (Wheldon et al., 2010), whereas the Xflrt3 intracellular region plays a key role in regulating cell de-adhesion during gastrulation via interactions with its cytoplasmic partner, the small GTPase Rnd1 (Ogata et al., 2007; Karaulanov et al., 2009; Chen et al., 2009). This association leads to localized downregulation of C-cadherin to promote cell

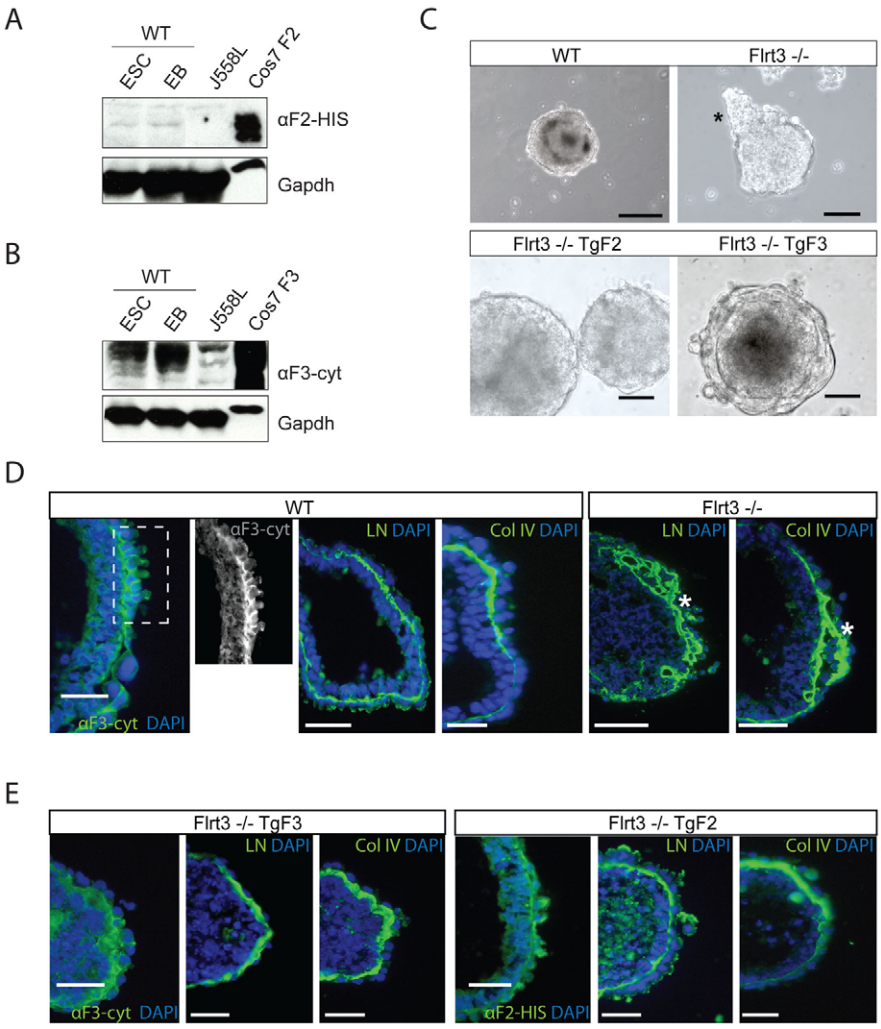

Fig. 7. *Flrt2* expression corrects the basement membrane defects in *Flrt3*-deficient embryoid bodies. (**A**,**B**) Western blot analysis shows that Flrt3 is strongly expressed by wild-type embryonic stem cells (ESCs) and embryoid bodies (EBs) (day7), while Flrt2 expression is present only at negligible levels. Cos7 cells transfected with a pCAGGS-*Flrt2* and *HAFlrt3* expression vectors serve as positive controls. J558L plasmacytoma cells that express no *Flrt2* and only low levels of *Flrt3* provide a negative control. (**C**) Phase-contrast photographs of representative day 7 wild-type, *Flrt3*$^{-/-}$, *Flrt3*$^{-/-}$*tgHAFlrt3* and *Flrt3*$^{-/-}$*tgFlrt2* EBs. Wild-type EBs form compact regular structures invested in a layer of primitive endoderm. By contrast, *Flrt3*$^{-/-}$ ESCs display marked protrusions (asterisk), owing to holes in the primitive endoderm layer. Expression of either *tgHAFlrt3* or *tgFlrt2* restores the morphology to wild type. Scale bars: 100 μm. (**D**) Endogenous Flrt3 was basolaterally expressed in the visceral endoderm. Wild-type d7 EBs immunostained for laminin (LN) and collagen IV (Col IV) display a thin and uniform BM layer compared with *Flrt3*$^{-/-}$ EBs where the BM is highly disorganized (asterisks). (**E**) Ectopic expression of either *tgHAFlrt3* or *tgFlrt2* rescues the organization of the BM. Scale bars: 50 μm.

movements. Thus, considerable evidence suggests that Flrt family proteins act as multifunctional cell-surface receptors guiding tissue morphogenesis at early stages of vertebrate development.

Flrt3 is the earliest and most strongly expressed family member in the developing mouse embryo (Maretto et al., 2008). Flrt3 plays an essential role in the AVE to localize signals that prevent mesoderm induction and establish anterior identity correctly to the underlying epiblast (Egea et al., 2008). Loss of *Flrt3* results in BM disorganization and disrupts the cell contacts that normally maintain this key morphogenetic boundary. Aberrant gastrulation in *Flrt3* mutants (Egea et al., 2008) secondarily results in a wide range of tissue disturbances, including abnormal ventral closure, headfold fusion and definitive endoderm migration (Egea et al., 2008; Maretto et al., 2008).

Flrt2 expression has a delayed onset in the AVE but by midgestation its expression broadly overlaps with *Flrt3*. Here, we describe dynamically regulated expression of *Flrt2* and *Flrt3* in the developing heart. *Flrt2* and *Flrt3* are co-expressed in the cardiomyocytes and the epicardium cell populations that both originate from common *Nkx2.4*- and *Isl1*-positive progenitors generated during late gastrulation (Zhou et al., 2008b). *Flrt2* and *Flrt3* co-expression is detectable shortly after the cardiomyocytes fuse across the ventral midline to form the primitive heart tube. Similarly the PEO, a prominent cluster of cell cysts that forms just caudal and ventral to the heart tube, is marked by very robust *Flrt2* and *Flrt3* co-expression. However, 24 hours later as the epicardial cells spread across the surface of the ventricle, *Flrt3* expression is rapidly lost. In striking contrast, *Flrt2* expression is robustly maintained in the epicardium.

Consistent with this unique site of expression, *Flrt2* mutants arrest beginning at E11.5 due to cardiac insufficiency. Loss of *Flrt2* has no noticeable effect on the initial delamination, adhesion and spreading of epicardial cells, but beginning at around E10.5 and coincident with downregulated expression of *Flrt3*, integrity of the epicardial sheet becomes severely compromised. Discontinuities appear in the ruffled epicardium and areas of detachment are associated with a localized thickening of the BM. These abnormal cell-cell contacts probably impair local trafficking of trophic factors synthesized by the epicardium to the adjacent myocytes. The marked failure in growth and expansion of the compact ventricular myocardium leads to decreased trabeculation and reduced endocardium. Considering that the trabeculae provide much of the additional contractile force required for increased circulation, coincident with the dramatic growth of the embryo at this stage of development, a strong argument can be made that severely compromised cardiac function accounts for the rapid onset lethality.

Recent experiments demonstrate that connexin 43-deficient epicardial cells also exhibit localized detachment from the ECM and form similar superficial ‘blisters’ (Rhee et al., 2009). However, connexin 43 seems to function in organizing cell polarity and

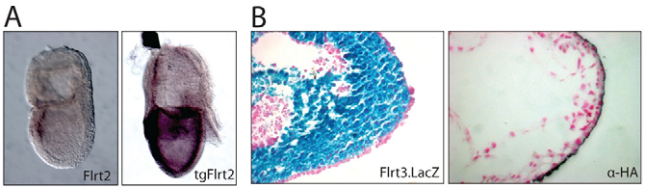

Fig. 8. Ectopic expression of *Flrt2* and HA-tagged *Flrt3* in transgenic mouse strains rescues embryonic lethality of *Flrt3*- and *Flrt2*-deficient embryos. (**A**) Endogenous *Flrt2* mRNA is confined to the AVE at E7.5, whereas *tgFlrt2* is robustly expressed throughout the entire embryonic region. (**B**) Endogenous *Flrt3.lacZ* expression is confined to the cardiomyocytes in E10.5 heart tissue, whereas HA immunostaining demonstrates tgHA-Flrt3 expression exclusively in the outermost epicardial layer.

coordinating directed epicardial cell migration into the myocardium. The present results demonstrate in explant cultures that *Flrt2* mutant epicardial cells migrate normally, but fail to form a tightly packed monolayer. Disrupted tissue integrity compromises the mechanical and signalling properties of the epicardium that collectively promote expansion of the compact ventricular myocyte layer.

The epicardium is known to be an essential source of secreted growth factors as well as cardiac progenitors (for a review, see Lavine and Ornitz, 2009). For example, physical or genetic ablation of the epicardium results in a thin ventricular myocardium. Loss of *Gata4*, which is known to be required for PEO specification (Watt et al., 2004), or *Par3*, which is essential for PEO cell delamination (Hirose et al., 2006) result in very early onset defects in the myocardium beginning at E9.5. Epicardial-derived factors including retinoic acid and Tgfβs regulate proliferation and maturation of the myocardium. Epicardial-specific inactivation of components of the retinoic acid signalling pathway, as well as of Alk5 (the TGFβ receptor), lead to underdevelopment of the ventricular myocytes and defective formation of the coronary vasculature (Chen et al., 2002; Sridurongrit et al., 2008; Merki et al., 2005).

Table 2. Genotyping results from tgFlrt2 and tgFlrt3 transgenic rescue intercross matings

A *tgFlrt2* expression rescues the majority of *Flrt3*$^{-/-}$ embryos*		
tg+Flrt2 : Flrt3$^{-/-}$	15	17%
tg+Flrt2 : Flrt3$^{+/-}$	43	50%
tg+Flrt2 : Flrt3$^{+/+}$	29	33%
Total tg^{+}	87	
tg-Flrt2 : Flrt3$^{-/-}$	7	7%
tg-Flrt2 : Flrt3$^{+/-}$	54	57%
tg-Flrt2 : Flrt3$^{+/+}$	34	36%
Total tg^{-}	95	
B *tgHA-Flrt3* expression rescues the majority of *Flrt2*$^{-/-}$ embryos†		
tg+Flrt3 : Flrt2$^{-/-}$	9	13%
tg+Flrt3 : Flrt2$^{+/-}$	40	58%
tg+Flrt3 : Flrt2$^{+/+}$	20	29%
Total tg^{+}	69	
tg-Flrt3 : Flrt2$^{-/-}$	0	0%
tg-Flrt3 : Flrt2$^{+/-}$	35	58%
tg-Flrt3 : Flrt2$^{+/+}$	25	42%
Total tg^{-}	60	

In both experiments, animals were genotyped at weaning.
*182 animals.
†129 animals.

Cell lineage tracing experiments have suggested that the epicardium not only provides a physical support tissue for the adjacent cardiomyocytes but also acts as a source of mature cell types, including smooth muscle cells and interstitial fibroblasts (for a review, see Winter and Gittenberger-de Groot, 2007). However, in contrast to previous observations in chick (for a review, see Ishii et al., 2010), mouse epicardial derivatives do not give rise to the coronary vessel endothelium. Rather, the initial vascular plexus, derived from angiogenic sprouts originating in the sinus venosus, migrates into the dorsal myocardium and gradually becomes reprogrammed to form the coronary vessel endothelium (Red-Horse et al., 2010). A subset of the epicardial cells undergo EMT and invade the myocardium differentiate to form smooth muscle cells of the coronary arteries (Merki et al., 2005; Cai et al., 2008; Zhou et al., 2008a; Red-Horse et al., 2010). The present results demonstrate that early vasculogenesis proceeds normally in the absence of *Flrt2*. However, owing to the early onset lethality at present, it remains unclear whether *Flrt2* may also function at later stages to promote epicardial de-adhesion, EMT and/or migration into the myocardium.

Additionally, Flrt2 and/or Flrt3 could potentially regulate development of the cardiomyocyte lineage. Double conditional deletions may also be required to test this possibility. However, the cardiac insufficiency phenotype observed here reflects Flrt2/3 essential requirements in the epicardium, as ectopic Flrt3 expression in transgenic embryos is sufficient to by-pass the lethality.

Fgfr1 signalling contributes to the expansion of the ventricular myocardium during the second half of gestation (Lavine et al., 2005). However, here we observe that *Flrt2* functional loss has no effect on phospho-Erk1/2 levels. Additionally, as for *Flrt3* (Maretto et al., 2008), Fgf inhibitors have no noticeable effect on *Flrt2* expression. These results strongly suggest that *Flrt2* functional activities are independent of Fgf signalling. Interestingly, an unbiased systematic protein interaction screen in zebrafish that examined all known leucine-rich repeat cell-surface proteins failed to detect interactions between the Flrt paralogues and members of the Fgfr family (Sollner and Wright, 2009). Rather, zebrafish Flrt extracellular LRR domains specifically bind to the Unc5b receptor. An interesting possibility is that mammalian Flrts, which are abundantly expressed in the brain (Lacy et al., 1999), also interact with Unc5b to guide neuronal migration. In the case of two closely related LRR transmembrane proteins, Tartan and Capricious, that establish tissue boundaries in the developing wing disc in *Drosophila*, cell sorting depends on both the extracellular LRR domain and cytoplasmic regions (Milan et al., 2005). Much additional work will be needed to understand how the extracellular recognition events mediated by Flrt proteins regulate signalling across cell-cell contacts in mammalian embryos.

The cardiac insufficiency phenotype in *Flrt2* mutants can best be explained due to focal defects in the epicardium. Thus, epicardial expression of *Flrt3* in transgenic embryos is sufficient to rescue the *Flrt2* lethal phenotype. Moreover, the BM disorganization and the failure to maintain epicardial tissue integrity caused by loss of *Flrt2* phenocopies those in the AVE of *Flrt3* mutants. Remarkably, *Flrt2* can functionally substitute for *Flrt3* in ES cell-derived EBs and transgenic embryos. Rescue in vivo is incompletely penetrant, possibly owing to non-physiological transgene expression levels. Nonetheless, these findings demonstrate that closely related Flrt2 and Flrt3 proteins can function interchangeably at these unique sites of expression. The widespread and overlapping dynamic Flrt2 and Flrt3

expression patterns suggest they may also modulate functional activities elsewhere. It is tempting to speculate that associations with diverse protein partners may serve to regulate cell movements and signalling. Conditional inactivation strategies will be required to test this possibility. The present studies demonstrate in the context of two different epithelial sheets – the visceral endoderm and the epicardium – that Flrt proteins play essential roles in maintaining cell-cell contacts. It will be important to characterize Flrt interaction networks that maintain tissue integrity within these developmentally important signalling centres.

Acknowledgements
We thank Emily Lejsek for generating the transgenic mice, Radu Ariescu for providing recombinant HIS-tagged Flrt2 protein, Mike Shaw and the Dunn School Imaging Facility for SEM, Janet Rossant for the Flt1.lacZ and Flk1.lacZ mice, and Ken Cho for the Flrt3 polyclonal antibody. This work was supported by a studentship from the MRC (P.M.) and by a Programme Grant from the Wellcome Trust (E.J.R.). E.J.R. is a Wellcome Trust Principal Research Fellow. Deposited in PMC for release after 6 months.

Competing interests statement
The authors declare no competing financial interests.

Supplementary material
Supplementary material for this article is available at
http://dev.biologists.org/lookup/suppl/doi:10.1242/dev.059386/-/DC1

References

Aricescu, A. R., Assenberg, R., Bill, R. M., Busso, D., Chang, V. T., Davis, S. J., Dubrovsky, A., Gustafsson, L., Hedfalk, K., Heinemann, U. et al. (2006a). Eukaryotic expression: developments for structural proteomics. *Acta Crystallogr. D Biol. Crystallogr.* **62**, 1114-1124.
Aricescu, A. R., Lu, W. and Jones, E. Y. (2006b). A time- and cost-efficient system for high-level protein production in mammalian cells. *Acta Crystallogr. D Biol. Crystallogr.* **62**, 1243-1250.
Armstrong, J. F., Pritchard-Jones, K., Bickmore, W. A., Hastie, N. D. and Bard, J. B. (1993). The expression of the Wilms' tumour gene, WT1, in the developing mammalian embryo. *Mech. Dev.* **40**, 85-97.
Austin, A. F., Compton, L. A., Love, J. D., Brown, C. B. and Barnett, J. V. (2008). Primary and immortalized mouse epicardial cells undergo differentiation in response to TGFbeta. *Dev. Dyn.* **237**, 366-376.
Bell, J. K., Mullen, G. E., Leifer, C. A., Mazzoni, A., Davies, D. R. and Segal, D. M. (2003). Leucine-rich repeats and pathogen recognition in Toll-like receptors. *Trends Immunol.* **24**, 528-533.
Bottcher, R. T., Pollet, N., Delius, H. and Niehrs, C. (2004). The transmembrane protein XFLRT3 forms a complex with FGF receptors and promotes FGF signalling. *Nat. Cell Biol.* **6**, 38-44.
Buckingham, M., Meilhac, S. and Zaffran, S. (2005). Building the mammalian heart from two sources of myocardial cells. *Nat. Rev. Genet.* **6**, 826-835.
Cai, C. L., Martin, J. C., Sun, Y., Cui, L., Wang, L., Ouyang, K., Yang, L., Bu, L., Liang, X., Zhang, X. et al. (2008). A myocardial lineage derives from Tbx18 epicardial cells. *Nature* **454**, 104-108.
Carson, C. T., Kinzler, E. R. and Parr, B. A. (2000). Tbx12, a novel T-box gene, is expressed during early stages of heart and retinal development. *Mech. Dev.* **96**, 137-140.
Chen, T. H., Chang, T. C., Kang, J. O., Choudhary, B., Makita, T., Tran, C. M., Burch, J. B., Eid, H. and Sucov, H. M. (2002). Epicardial induction of fetal cardiomyocyte proliferation via a retinoic acid-inducible trophic factor. *Dev. Biol.* **250**, 198-207.
Chen, X., Koh, E., Yoder, M. and Gumbiner, B. M. (2009). A protocadherin-cadherin-FLRT3 complex controls cell adhesion and morphogenesis. *PLoS One* **4**, e8411.
Dunn, N. R., Koonce, C. H., Anderson, D. C., Islam, A., Bikoff, E. K. and Robertson, E. J. (2005). Mice exclusively expressing the short isoform of Smad2 develop normally and are viable and fertile. *Genes Dev.* **19**, 152-163.
Egea, J., Erlacher, C., Montanez, E., Burtscher, I., Yamagishi, S., Hess, M., Hampel, F., Sanchez, R., Rodriguez-Manzaneque, M. T., Bosl, M. R. et al. (2008). Genetic ablation of FLRT3 reveals a novel morphogenetic function for the anterior visceral endoderm in suppressing mesoderm differentiation. *Genes Dev.* **22**, 3349-3362.
Fong, G. H., Rossant, J., Gertsenstein, M. and Breitman, M. L. (1995). Role of the Flt-1 receptor tyrosine kinase in regulating the assembly of vascular endothelium. *Nature* **376**, 66-70.
Haines, B. P., Wheldon, L. M., Summerbell, D., Heath, J. K. and Rigby, P. W. (2006). Regulated expression of FLRT genes implies a functional role in the regulation of FGF signalling during mouse development. *Dev. Biol.* **297**, 14-25.
Hirose, T., Karasawa, M., Sugitani, Y., Fujisawa, M., Akimoto, K., Ohno, S. and Noda, T. (2006). PAR3 is essential for cyst-mediated epicardial development by establishing apical cortical domains. *Development* **133**, 1389-1398.
Ishii, Y., Garriock, R. J., Navetta, A. M., Coughlin, L. E. and Mikawa, T. (2010). BMP signals promote proepicardial protrusion necessary for recruitment of coronary vessel and epicardial progenitors to the heart. *Dev. Cell* **19**, 307-316.
Jiang, X., Rowitch, D. H., Soriano, P., McMahon, A. P. and Sucov, H. M. (2000). Fate of the mammalian cardiac neural crest. *Development* **127**, 1607-1616.
Karaulanov, E., Bottcher, R. T., Stannek, P., Wu, W., Rau, M., Ogata, S., Cho, K. W. and Niehrs, C. (2009). Unc5B interacts with FLRT3 and Rnd1 to modulate cell adhesion in Xenopus embryos. *PLoS One* **4**, e5742.
Karaulanov, E. E., Bottcher, R. T. and Niehrs, C. (2006). A role for fibronectin-leucine-rich transmembrane cell-surface proteins in homotypic cell adhesion. *EMBO Rep.* **7**, 283-290.
Kobe, B. and Kajava, A. V. (2001). The leucine-rich repeat as a protein recognition motif. *Curr. Opin. Struct. Biol.* **11**, 725-732.
Koonce, C. H. and Bikoff, E. K. (2004). Dissecting MHC class II export, B cell maturation, and DM stability defects in invariant chain mutant mice. *J. Immunol.* **173**, 3271-3280.
Kraus, F., Haenig, B. and Kispert, A. (2001). Cloning and expression analysis of the mouse T-box gene Tbx18. *Mech. Dev.* **100**, 83-86.
Kwee, L., Baldwin, H. S., Shen, H. M., Stewart, C. L., Buck, C., Buck, C. A. and Labow, M. A. (1995). Defective development of the embryonic and extraembryonic circulatory systems in vascular cell adhesion molecule (VCAM-1) deficient mice. *Development* **121**, 489-503.
Lacy, S. E., Bonnemann, C. G., Buzney, E. A. and Kunkel, L. M. (1999). Identification of FLRT1, FLRT2, and FLRT3: a novel family of transmembrane leucine-rich repeat proteins. *Genomics* **62**, 417-426.
Lavine, K. J. and Ornitz, D. M. (2009). Shared circuitry: developmental signaling cascades regulate both embryonic and adult coronary vasculature. *Circ. Res.* **104**, 159-169.
Lavine, K. J., Yu, K., White, A. C., Zhang, X., Smith, C., Partanen, J. and Ornitz, D. M. (2005). Endocardial and epicardial derived FGF signals regulate myocardial proliferation and differentiation in vivo. *Dev. Cell* **8**, 85-95.
Lu, X., Le Noble, F., Yuan, L., Jiang, Q., De Lafarge, B., Sugiyama, D., Breant, C., Claes, F., De Smet, F., Thomas, J. L. et al. (2004). The netrin receptor UNC5B mediates guidance events controlling morphogenesis of the vascular system. *Nature* **432**, 179-186.
Manner, J., Perez-Pomares, J. M., Macias, D. and Munoz-Chapuli, R. (2001). The origin, formation and developmental significance of the epicardium: a review. *Cells Tissues Organs* **169**, 89-103.
Maretto, S., Müller, P. S., Aricescu, A. R., Cho, K. W., Bikoff, E. K. and Robertson, E. J. (2008). Ventral closure, headfold fusion and definitive endoderm migration defects in mouse embryos lacking the fibronectin leucine-rich transmembrane protein FLRT3. *Dev. Biol.* **318**, 184-193.
Martin-Puig, S., Wang, Z. and Chien, K. R. (2008). Lives of a heart cell: tracing the origins of cardiac progenitors. *Cell Stem Cell* **2**, 320-331.
Merki, E., Zamora, M., Raya, A., Kawakami, Y., Wang, J., Zhang, X., Burch, J., Kubalak, S. W., Kaliman, P., Belmonte, J. C. et al. (2005). Epicardial retinoid X receptor alpha is required for myocardial growth and coronary artery formation. *Proc. Natl. Acad. Sci. USA* **102**, 18455-18460.
Milan, M., Perez, L. and Cohen, S. M. (2005). Boundary formation in the Drosophila wing: functional dissection of Capricious and Tartan. *Dev. Dyn.* **233**, 804-810.
Nagy, A. (2003). *Manipulating the Mouse Embryo: A Laboratory Manual, 3rd Edn*. Cold Spring Harbor, N.Y.: Cold Spring Harbor Laboratory Press.
Niwa, H., Yamamura, K. and Miyazaki, J. (1991). Efficient selection for high-expression transfectants with a novel eukaryotic vector. *Gene* **108**, 193-199.
Ogata, S., Morokuma, J., Hayata, T., Kolle, G., Niehrs, C., Ueno, N. and Cho, K. W. (2007). TGF-beta signaling-mediated morphogenesis: modulation of cell adhesion via cadherin endocytosis. *Genes Dev.* **21**, 1817-1831.
Olson, E. N. (2006). Gene regulatory networks in the evolution and development of the heart. *Science* **313**, 1922-1927.
Ong, S. H., Dilworth, S., Hauck-Schmalenberger, I., Pawson, T. and Kiefer, F. (2001). ShcA and Grb2 mediate polyoma middle T antigen-induced endothelial transformation and Gab1 tyrosine phosphorylation. *EMBO J.* **20**, 6327-6336.
Red-Horse, K., Ueno, H., Weissman, I. L. and Krasnow, M. A. (2010). Coronary arteries form by developmental reprogramming of venous cells. *Nature* **464**, 549-553.
Rhee, D. Y., Zhao, X. Q., Francis, R. J., Huang, G. Y., Mably, J. D. and Lo, C. W. (2009). Connexin 43 regulates epicardial cell polarity and migration in coronary vascular development. *Development* **136**, 3185-3193.
Robertson, E. J. (1987). *Teratocarcinomas and Embryonic Stem Cells: A Practical Approach*. Oxford: IRL.
Sengbusch, J. K., He, W., Pinco, K. A. and Yang, J. T. (2002). Dual functions of alpha4beta1 integrin in epicardial development: initial migration and long-term attachment. *J. Cell Biol.* **157**, 873-882.
Shalaby, F., Rossant, J., Yamaguchi, T. P., Gertsenstein, M., Wu, X. F., Breitman, M. L. and Schuh, A. C. (1995). Failure of blood-island formation and vasculogenesis in Flk-1-deficient mice. *Nature* **376**, 62-66.

Smith, T. G. and Tickle, C. (2006). The expression of Flrt3 during chick limb development. *Int. J. Dev. Biol.* **50**, 701-704.
Sollner, C. and Wright, G. J. (2009). A cell surface interaction network of neural leucine-rich repeat receptors. *Genome Biol.* **10**, R99.
Sridurongrit, S., Larsson, J., Schwartz, R., Ruiz-Lozano, P. and Kaartinen, V. (2008). Signaling via the Tgf-beta type I receptor Alk5 in heart development. *Dev. Biol.* **322**, 208-218.
Srivastava, D. and Olson, E. N. (2000). A genetic blueprint for cardiac development. *Nature* **407**, 221-226.
Stennard, F. A., Costa, M. W., Lai, D., Biben, C., Furtado, M. B., Solloway, M. J., McCulley, D. J., Leimena, C., Preis, J. I., Dunwoodie, S. L. et al. (2005). Murine T-box transcription factor Tbx20 acts as a repressor during heart development, and is essential for adult heart integrity, function and adaptation. *Development* **132**, 2451-2462.
Sucov, H. M. (1998). Molecular insights into cardiac development. *Annu. Rev. Physiol.* **60**, 287-308.
Vincent, S. D. and Buckingham, M. E. (2010). How to make a heart: the origin and regulation of cardiac progenitor cells. *Curr. Top. Dev. Biol.* **90**, 2-41.
Vincent, S. D., Norris, D. P., Le Good, J. A., Constam, D. B. and Robertson, E. J. (2004). Asymmetric Nodal expression in the mouse is governed by the combinatorial activities of two distinct regulatory elements. *Mech. Dev.* **121**, 1403-1415.
Watt, A. J., Battle, M. A., Li, J. and Duncan, S. A. (2004). GATA4 is essential for formation of the proepicardium and regulates cardiogenesis. *Proc. Natl. Acad. Sci. USA* **101**, 12573-12578.
Wheldon, L. M., Haines, B. P., Rajappa, R., Mason, I., Rigby, P. W. and Heath, J. K. (2010). Critical role of FLRT1 phosphorylation in the interdependent regulation of FLRT1 function and FGF receptor signalling. *PLoS One* **5**, e10264.
Winter, E. M. and Gittenberger-de Groot, A. C. (2007). Epicardium-derived cells in cardiogenesis and cardiac regeneration. *Cell. Mol. Life Sci.* **64**, 692-703.
Yang, J. T., Rayburn, H. and Hynes, R. O. (1995). Cell adhesion events mediated by alpha 4 integrins are essential in placental and cardiac development. *Development* **121**, 549-560.
Zhou, B., Ma, Q., Rajagopal, S., Wu, S. M., Domian, I., Rivera-Feliciano, J., Jiang, D., von Gise, A., Ikeda, S., Chien, K. R. et al. (2008a). Epicardial progenitors contribute to the cardiomyocyte lineage in the developing heart. *Nature* **454**, 109-113.
Zhou, B., von Gise, A., Ma, Q., Rivera-Feliciano, J. and Pu, W. T. (2008b). Nkx2-5- and Isl1-expressing cardiac progenitors contribute to proepicardium. *Biochem. Biophys. Res. Commun.* **375**, 450-453.